Behavior of Railroad Bridge Girders Due to Brake Loads with LISA V.8 FEA

Aco Wahyudi Efendi(✉)

Universitas Tridharma, Jl. A.W. Syahrani No.7, Batu Ampar, Balikpapan Utara, Balikpapan 76126, Indonesia
aw.efendi2018@gmail.com

Abstract. The railroad track is very important as a means of crossing the train itself, especially for lines that have a fairly extreme elevation, where for the railroad itself it is not allowed to have a track with a very high grid.

This study uses the finite element method with assistance from LISA V.8 FEA(License), a finite element method software package, to examine the stresses that develop on railroad track girder bridges in comparison to the stresses that develop on each component, including rails, sleepers, and the bridge girder itself, as a result of rail traffic loads and brake impact loads between the railroad tracks and the railroad wheels.

According to the results of the analysis of the stress distribution behavior that happens on the railroad track girder bridge with two types of loading, namely the service load and the shock/brake load, the starting stress that occurs due to the service load is 32.91 N/mm2 and the increase in stress that occurs due to the brake load is 58.85 N/mm2. The service load causes a stress distribution on the bridge girder of 9.39 N/mm2, and the brake load causes a stress distribution of 16.76 N/mm2. Whereas the ratio of the increase in stress on the railroad is 1.788, and the ratio of the increase in stress on the bridge girder is 1.784.

Keywords: FEM · Girder · LISA · Railroad · Stress

1 Introduction

The railroad track is very important as a means of crossing the train itself, especially for lines that have a fairly extreme elevation, where for the railroad itself it is not allowed to have a track with a very high grid. Literally, a bridge is a structure that functions as a link between two parts that are separated by an obstacle, both natural such as rivers, valleys, and straits or the sea, or artificial such as roads, irrigation canals, and railroads [1].

Bridges come in a variety of designs, materials, and functions in the world of building, and these factors can be taken into account while deciding on the sort of bridge to utilize. In light of this, the choice The concrete-primarily constructed bridge intends to build a robust, rigid, and water-resistant structure that will be suited for bridge building with long-term plans [2].

W. A. Wirawan et al. (Eds.): ICORT 2022, AER 220, pp. 24–38, 2023.
https://doi.org/10.2991/978-94-6463-126-5_4

Structurally the girder bridge has its own advantages and disadvantages depending on the materials to be used, and also provide time and cost efficiencies. With the advent of modern railroads, rail-bridge interaction has grown to be a crucial component of rail and bridge design. Since this movement might cause the bridge to bend like a traffic load, the influence of the temperature difference on the bridge is significant and cannot be disregarded [3].

This study uses the finite element method with assistance from LISA V.8 FEA(License), a finite element method software package, to examine the stresses that develop on railroad track girder bridges in comparison to the stresses that develop on each component, including rails, sleepers, and the bridge girder itself, as a result of rail traffic loads and brake impact loads.

2 Research Method

This study uses the finite element analysis program LISA FEA V.8 to do model analysis. The author will model the railroad that is above the girder of the track bridge to the stress behavior due to the load that occurs and the brake force that occurs on the railroad. Based on two components of the train lines.

The Regulation of the Minister of Transport of the Republic of Indonesia No. PN. 60 of 2012 on the technical standards for the railway line applies to the size of the railway bearing. The use and installation of a normal 1435mm rail width railway in a specified cant location [2, 4, 5]

According to Figure 1, the rail structure is created as well as possible to be able to withstand heavy loads, or the term AXLE LOAD, of the train series running on it. This way, the steel road can survive for a long time and the train series may travel quickly, safely, and comfortably.

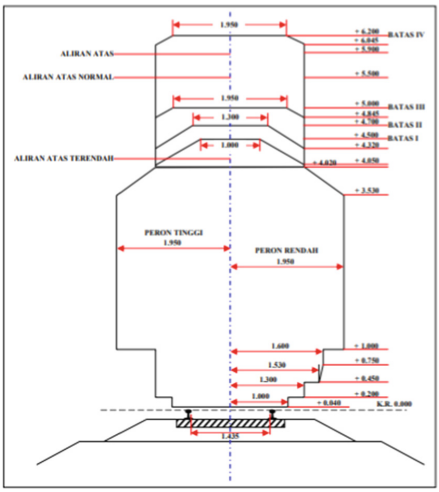

Fig. 1. The position of laying the railroad tracks on the bearings

Fig. 2. Railroad concrete bearing

2.1 Bearing Railroad

The bearing keeps the railroad's width and stability on the outside of the rail by transferring the weight of the railroad structure and the rail load to the ballast.

Concrete, steel/iron, or wood can all be used to create bearings. The diversity, field conditions, and availability all factor into the decision of storage type. Each bearing type's specifications must make reference to the relevant technical specifications.

For a rail width of 1067 mm, the prestressed steel must have a minimum tensile strength of 16.876 kg/cm2 and must have a concrete compressive strength of at least 500 kg/cm2 (1.655 MPa). Concrete bearings must have a minimum moment absorption capacity of 1500 kg/m at the rail seat and the middle of the bearing weighs -930 kgm. For a rail width of 1435 mm, the quality of the prestressed steel must have a minimum tensile strength of 16.876 kg/cm 2 and a characteristic concrete compressive strength of at least 600 kg/cm2 (1.655 MPa). Concrete bearings must be able to absorb the least amount of moments, depending on the design of the axle load and speed.

2.2 Rail

A. Rails must adhere to the following standards:

1. 10% or more of an elongation;
2. at least 1175 N/mm2 in terms of tensile strength;
3. The rail head's hardness shouldn't be less than 320 BHN.

According to the chart and the following Fig. 3, the rail cross-section must match the rail measurements.:

The explanation of the symbol above is

A = cross-sectional area

W= rail weight per meter

I_x= moment of inertia about the x-axis

Y_b= the distance from the bottom of the rail to the neutral line

The maximum pressure (axle load) the rail can withstand during a train pass as well as the permitted speed of the train as it passes the rail are both impacted by the various types of rail rod. The axle load that the rail can support increases with increasing "R," allowing trains to go over it safely and steadily at high speeds.[4].

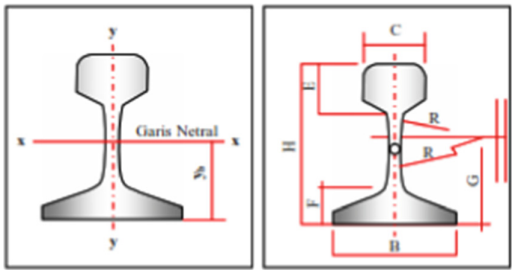

Fig. 3. Rail dimensions

Table 1. - Rail Section Dimensions.

Geometric size	Rail Type			
	R 42	R 50	R 54	R 60
H (mm)	138.00	153.00	159.00	172.00
B (mm)	110.00	127.00	140.00	150.00
C (mm)	68.50	65.00	70.00	74.30
D (mm)	13.50	15.00	16.00	16.50
E (mm)	40.50	49.00	49.40	51.00
F (mm)	23.50	30.00	30.20	31.50
G (mm)	72.00	76.00	74.79	80.95
R (mm)	320.00	500.00	508.00	120.00
A (cm^2)	54.26	64.20	69.34	76.86
W (kg/m)	42.59	50.40	54.43	60.34
I_x (cm^4)	1,369.00	1,960.00	2,346.00	3,055.00
Y_b (mm)	68.50	71.60	76.20	80.95

2.3 Railway Components

After the foundation layer is completed as the foundation of the railway, the next stage is to build the railway tracks. Please note that each component affects the quality of the railway itself. Figure 4 shows a railroad schematic and its components.

2.4 Steel Girder

A steel girder bridge, also known as a composite steel girder bridge, is made of common steel parts that are bolted together. Standard steel girder bridges have class A and class B spans that are 20 m, 25 m, and 30 m lengthy.

The fundamental component of the railroad's infrastructure and a feature of the rail mode of transportation that links the train from one place to another is the Railway Bridge. For the time being, truss bridges are the norm for choosing materials for railway bridges.

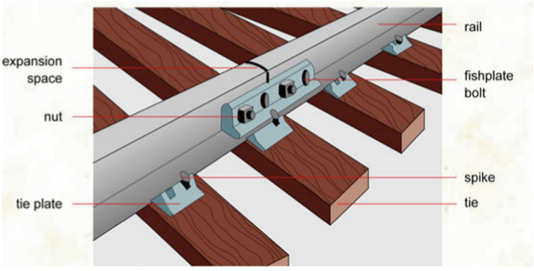

Fig. 4. Railroad track components (source: www.infovisual.info)

Fig. 5. Railroad track components (source: https://jateng.antaranews.com/berita/360664/jembatan-kereta-api-di-brebes-gogos-perjalanan-ka-daop-5-purwokerto-terganggu)

In addition to being simple to transport, steel materials are also simple to assemble since they adhere to the selection standards for steel bridges. Useful, simple to construct, check, maintain, effective, and able to adapt to the construction environment. There are two categories of railroad steel bridges:

1. Wall Through Truss (WTT); spans of 35, 42, 51, 76, and 100 m.
2. Wall Through Plate (WTP) with spans of 11, 15, 21, and 31 m

The dimensions of the steel girder used on the railway track bridge are WF 1200.450.20.38 with the following parameters Fig. 5.

2.5 Finite Element Method (FEM)

Using a numerical approach, the finite element method (FEM) can be used to solve technical analytical issues. To create equations for a linear or nonlinear system, the finite element method incorporates various mathematical ideas. Over 20,000 equations are frequently generated, which is a very high number. Therefore, unless a suitable computer is used, this method has little practical value [6]–[11].

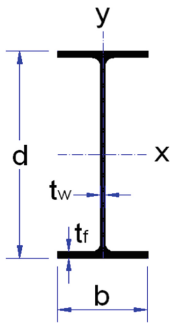

Fig. 6. Steel Profile

Table 2. – Bridge girder dimensions.

STEEL PROFILE :	WF 1200.450.20.38		
Steel profile weight,	W_{profil} =	3.8844	kN/m
Tinggi,	d =	1,200	mm
Width,	b =	450	mm
body thickness,	tw =	20	mm
wing thickness,	tf =	38	mm
	r =	22	mm
Cross-sectional area,	A =	49,800	mm2
Moment resistance,	Wx =	19,518,900	mm3
	Wy =	2,028,378	mm3
Moment of inertia,	Ix =	11,711,340,000	mm4
	Iy =	456,385,000	mm4
	rx =	485	mm
	ry =	96	mm
Girder span length,	L =	20,000	mm
Concrete slab thickness,	h =	200	mm

Strain (deformation), stress, temperature, pressure, and flow rate are produced when a structure is subjected to forces like stress, pressure, temperature, flow rate, and heat. The characteristics of the force and stress system itself determine how the ensuing action (deformation) is distributed throughout the body. You may find the distribution of this effect, given as displacement, using the finite element approach.

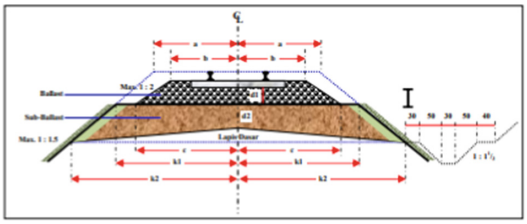

Fig. 7. Cross Section of Railroad in Straight Section

Finding the displacements of vertices, connections, lattices, and structural forces is a problem that is solved by the finite element method using an element discretization approach. The matrix method for structural analysis is related to discrete element equations, and the outcomes are the same as those of traditional structural analysis. One-dimensional (line elements), two-dimensional (plane elements), or three-dimensional (volume/continuum elements) discretization techniques are available. This method employs a continuum element to find a more accurate solution [12, 13]

2.6 LISA

Three distinct models of heat exchangers were utilized to evaluate the temperature rise using LISA, a well-known finite element analysis program. The line element model, the shell model, and the solid model are the three different sorts of models, in decreasing order of complexity and ease of fabrication.

LISA offers a selection of frequently used structural shapes for line elements, so users just need to enter the element's dimensions in one dialog box and its thermal conductivity in another.

Since we cannot completely rule out convection while creating the baseplate surface with the face selection tool, the convection coefficient of the baseplate surface must be set at half the value used elsewhere for line element models only. Just use common sense, actually.

It is simple to omit the mounting surface from convection for the other two models; we simply don't choose that surface. In each scenario, the volume of the entire floor slab is thought to be used as the heat source and an internal heat generator is utilised. Applying boundary conditions to a line element model calls for caution. When "Area" is selected, LISA chooses all surfaces of the line elements [14–20].

3 Results and Discussion

Figures 1 and 10 illustrate a typical scheme across railways under cant conditions, with the bearing railway state limited to conditions with a rail width of 1435 mm and a maximum height of 150 mm.

(Railway Width 1435 mm)

For a typical rail width as shown in Fig. 11.

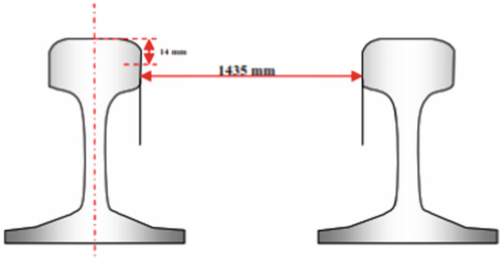

Fig. 8. Railway width 1435 mm

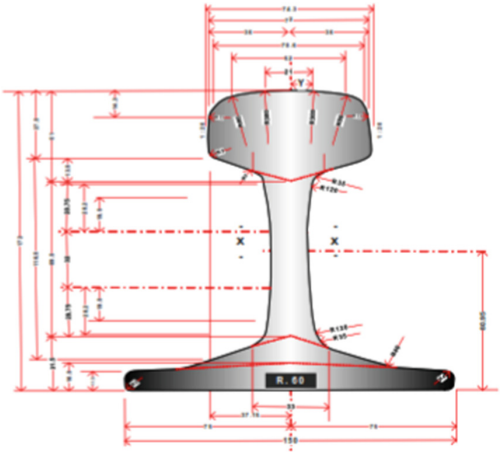

Fig. 9. Rail section size R.60

The maximum P-load of the axle is 22.5 tons when using the rail type, R.60 with the bearing type shown in Fig. 12, and for the three types of analysis used, steel, concrete, and wood, the distance between the bearing axes is 60 cm. The road class is limited to the rail class Type I with a load capacity >20.106 tons/year and a speed of 160 km/h.

3.1 Stress Behavior on Railroad Bridge Girders Due to Service Loads with LISA FEA

The position of the steel girder of the railroad track bridge is modeled in accordance with Figure 10, where the girder is symmetrically parallel to the position of the railroad tracks with a distance of 1509.3 mm and the dimensions of the concrete bearing used, the length of the bearing with the axle load above. is 2,740 mm 22.5 tonnes and has a maximum width of 330 m with a height under rail mount 220 mm. The maximum axial load, or 22.7 tons, is applied to the top surface of the rail, which has a width of 74.2 mm, dividing the load into 3032,345013 N/mm equally.

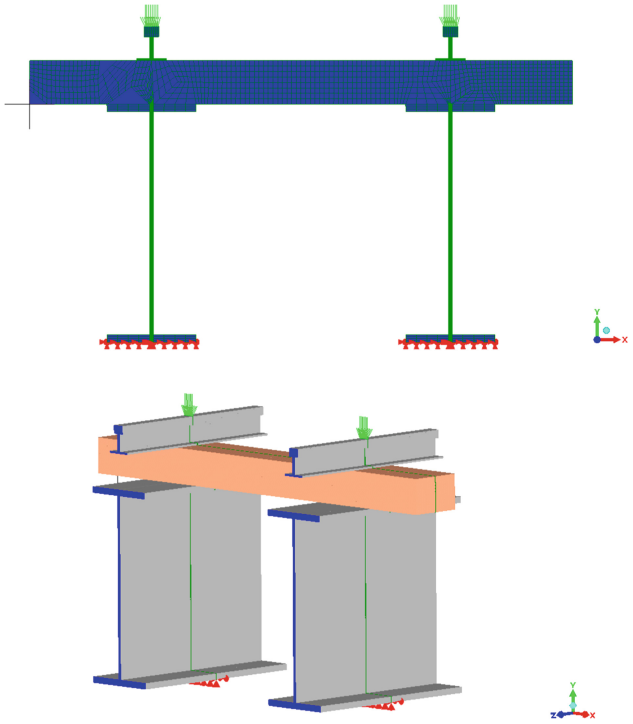

Fig. 10. Modeling of railroad track steel girder bridge with service load

From Figure 10 shows the pattern of loading on the cross-section of the railroad that is above the bridge girder and Figure 11(a) shows the pattern of stress distribution that occurs in the entire cross-section of the railroad track bridge.

It can be seen that a large stress occurs at the top of the rail surface, the greatest stress focuses on the meeting part of the rail head with the rail web itself because the load acts directly at the location of the rail surface, and the stress that occurs on the railroad is 32.91 N/mm^2 according to the Figure 11(b), on another element, namely railroad sleepers, also experience stress resulting from the stress distribution carried by the railroad and centered on the area where the bottom of the railroad meets the bearing, where a stress of 16.32 N/mm^2 occurs as seen in the Fig. 11(c) and on the impacted girder, the result of the stress distribution that occurs in the two elements above it is 9.39 N/mm^2 as shown in Figure 11(d).

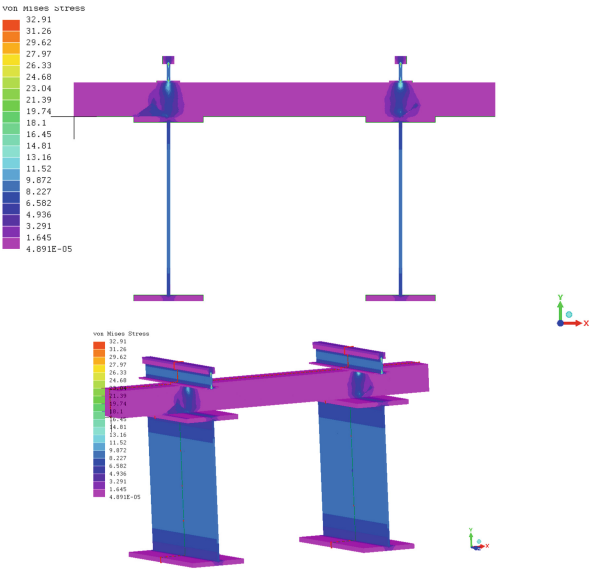

(a)

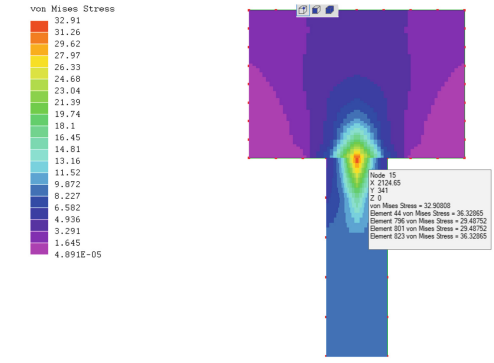

(b)

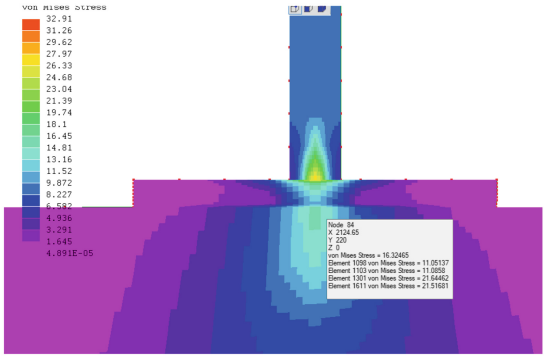

(c)

Fig. 11. (a) stress distribution behavior across the cross-section (b) the stress on the railroad tracks (c) stress that occurs in the rail bearing (d) stress on the bridge girder.

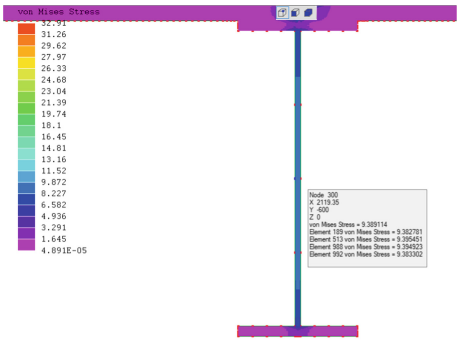

(d)

Fig. 11. (*continued*)

3.2 Stress Behavior on Railway Bridge Girders Due to Brake/Shock Loads with LISA FEA

The shock load is calculated by dividing the load vector by the factor i. The formula for railways directly on steel provides the most straightforward method for calculating factor I. Where i = shock factor, L = span length (m).

$$i = 0.3 + \frac{25}{50 + L}$$

The length of the span between the railroad tracks is 1200 mm, the value of the shock factor caused by the train brake is 0.788281, and the load on the rail surface is 3032 N/mm, where the load due to the shock factor is 2390.34 N/mm so the total load when the brake occurs is 5423 N/mm

It can be seen that a large stress occurs at the top of the rail surface, the greatest stress focuses on the meeting part of the rail head with the rail web itself because the load acts directly at the location of the rail surface, and the stress that occurs on the railroad is 58.85 N/mm^2 according to the Fig. 12(b), on another element, namely railroad sleepers, also experience stress resulting from the stress distribution carried by the railroad and centered on the area where the bottom of the railroad meets the bearing, where a stress of 22.94 N/mm^2 occurs as seen in the Fig. 12(c) and on the impacted girder, the result of the stress distribution that occurs in the two elements above it is 16.76 N/mm^2 as shown in Figure 12(d).

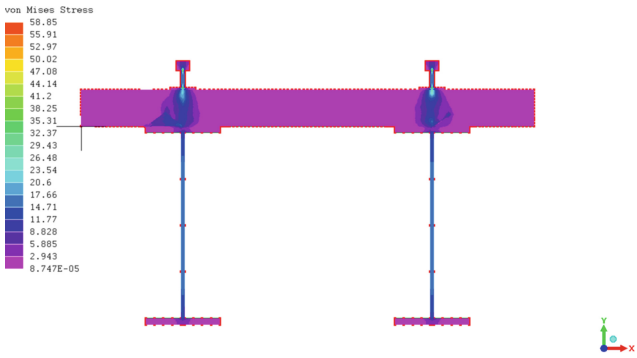

(a)

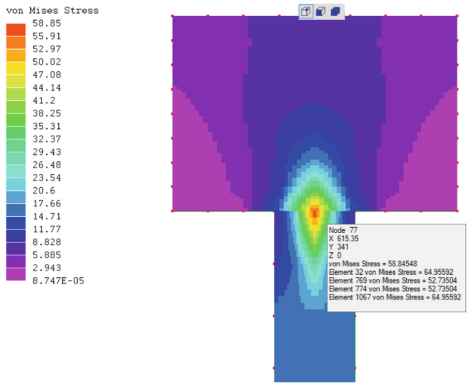

(b)

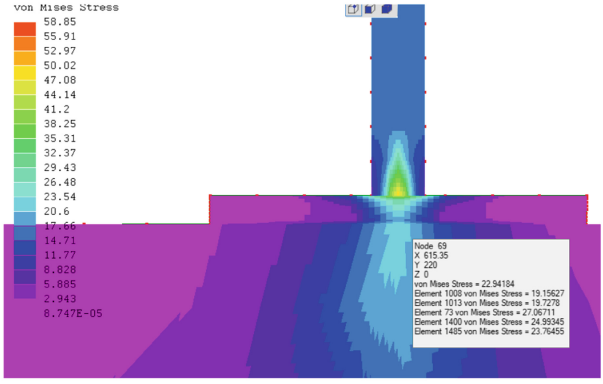

(c)

Fig. 12. (a) stress distribution behavior across the cross-section (b) the stress on the railroad tracks (c) stress that occurs in the rail bearing (d) stress on the bridge girder

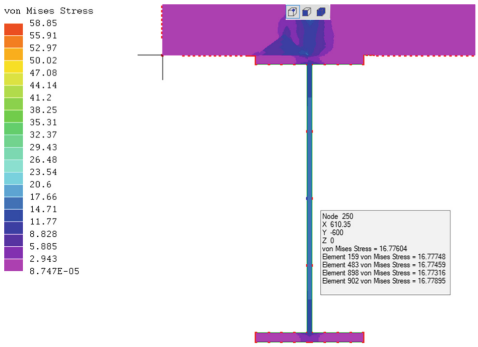

(d)

Fig. 12. (*continued*)

4 Conclusion

The stress that develops on the railroad track girder bridge under two separate loadings, namely the service load and the load from braking shock, is discovered using the Finite Element Analysis (FEA) modeling technique with LISA V.8 software. According to the results of the analysis of the stress distribution behavior that happens on the railroad track girder bridge with two types of loading, namely the service load and the shock/brake load, the starting stress that occurs due to the service load is 32.91 N/mm^2 and the increase in stress that occurs due to the brake load is 58.85 N/mm^2. The service load causes a stress distribution on the bridge girder of 9.39 N/mm^2, and the brake load causes a stress distribution of 16.76 N/mm^2. Whereas the ratio of the increase in stress on the railroad is 1.788, and the ratio of the increase in stress on the bridge girder is 1.784.

References

1. Supriyadi, B and Muntohar, A. S, Jembatan. Beta Offset, 2013.
2. Muspitasari, T, "Evaluasi peraturan pembebanan gandar kereta api di pulau Jawa terhadap kondisi aktual," Jurnal Teknik Sipil UAJY, vol. 14, no. 3, pp. 182–187, 2017, https://doi.org/10.24002/jts.v14i3.1982.
3. M. Su, Y. Yang, and R. Pan, "A comprehensively overall track-bridge interaction study on multi-span simply supported beam bridges with longitudinal continuous ballastless slab track," … Engineering and Mechanics, An Int'l Journal, 2021, [Online]. Available: https://www.dbpia.co.kr/Journal/articleDetail?nodeId=NODE10696911
4. Kementerial Perhubungan Republik Indonesia, Persyaratan Teknis Jalur Kereta Api, PM. 60. Kementerial Perhubungan Republik Indonesia, 2012.
5. F. Rozaq, W. Artha Wirawan, A. Zulkarnaen, Jamaluddin, and H. Boedi Wahjono, "The Influence of Temperature and Lubrication Variation on the Dimension Change in Ring Compression Test Using Ansys Software," J. Phys. Conf. Ser., vol. 1273, no. 1, 2019, https://doi.org/10.1088/1742-6596/1273/1/012080.

6. X. Chen, L. Pan, L. Xu, and C. Shi, "Three-Dimensional Vehicle–Curved Track Dynamic Model Based on FEM and DEM," … Journal of Structural Stability and …, 2021, https://doi.org/10.1142/S0219455421501790.
7. Z. Y. Wang, Y. F. Jin, Z. Y. Yin, and ..., "A novel coupled NS-PFEM with stable nodal integration and polynomial pressure projection for geotechnical problems," … Journal for Numerical and …, 2022, https://doi.org/10.1002/nag.3417.
8. H. M. Elsanadedy, Y. A. Al-Salloum, M. A. Alrubaidi, and ..., "Finite element analysis for progressive collapse potential of precast concrete beam-to-column connections strengthened with steel plates," Journal of Building …, 2021, [Online]. Available: https://www.sciencedirect.com/science/article/pii/S2352710220335087
9. P. M. Gullett, M. M. Dickey, and I. L. Howard, "Finite Element Analysis of Highway Bridges Subjected to Hurricane Storm Surge via the AMBUSH Framework," Journal of Bridge Engineering, 2020, https://doi.org/10.1061/%28ASCE%29BE.1943-5592.0001602.
10. W. D. Leslie, Y. Luo, S. Yang, A. L. Goertzen, and ..., "Fracture risk indices from DXA-based finite element analysis predict incident fractures independently from FRAX: The Manitoba BMD Registry," Journal of Clinical …, 2019, [Online]. Available: https://www.sciencedirect.com/science/article/pii/S1094695018302816
11. P. Singh and S. P. Harsha, "Finite Element Analysis of Cartridge Tapered Roller Bearing of Freight Wagon," International Journal of Vehicle Structures and …, 2018, [Online]. Available: http://ischolar.info/index.php/IJVSS/article/view/185330
12. T. M. Gondhalekar and S. K. Panigrahi, "Transient Analysis of Railway Sleeper using Three-Dimensional Finite Element Method," Journal of The Institution of Engineers …, 2021, https://doi.org/10.1007/s40030-021-00582-5.
13. W. Artha Wirawan, A. Zulkarnain, H. Boedi Wahjono, Jamaludin, and A. Tyas Damayanti, "The Effect of Material Exposure Variations on Energy Absorption Capability and pattern of Deformation Material of Crash Box of Three Segments," J. Phys. Conf. Ser., vol. 1273, no. 1, 2019, https://doi.org/10.1088/1742-6596/1273/1/012081.
14. A. W. Efendi, "Behavior of railroad bearing due to temperature and load using LISA FEA," Journal of Railway Transportation and Technology, 2022, [Online]. Available: https://jrtt.org/index.php/jrtt/article/view/1
15. A. W. Efendi, "Structural Design Tuak River Pedestrian Suspension Bridge Anchor Block Type Rigid Symmetric with LISA," Elektriese: Jurnal Sains dan Teknologi Elektro, 2022, [Online]. Available: https://jurnal.itscience.org/index.php/elektriese/article/view/1572
16. N. Akcay, A. S. Gökalp, A. Günlemez, and ..., "Comparison of LISA vs INSURE Tech-nique Using Nasal Intermittent Positive Pressure Ventilation (NIPPV) Support In Preterm Infants: A Randomized Controlled Trial.," Medical Journal of …, 2021, https://search.ebscohost.com/login.aspx?direct=true&profile=ehost&scope=site&authtype=crawler&jrnl=13059319&AN=150026811&h=oa0JPzH%2F7kU0O6pXKM9bccbhmpQED-KIgq3iXNk0ZUZxlRjSTzIU5R%2BKnLbrndMQP950wl66%2B7Ip5scAz0%2BViPA%3D%3D&crl=c
17. A. W. Efendi, "Behavior Analysis of Building Structures After a Fire with FEA LISA V. 8," Kurva S: Jurnal Keilmuan dan Aplikasi Teknik …, 2022, http://ejurnal.untag-smd.ac.id/index.php/TEKNIKD/article/view/6413
18. S. Widi Astuti, W. Artha Wirawan, A. Zulkarnain, and D. Tri Istiantara, "Comparison of Energy Absorption and Pattern of Deformation Material Crash Box of Three Segments with Bilinear and Johnson Cook Approach," J. Phys. Conf. Ser., vol. 1273, no. 1, 2019, https://doi.org/10.1088/1742-6596/1273/1/012078.

19. J. Fumagalli, M. Pieroni, S. Renaux-Petel, and ..., "Detecting primordial features with LISA," Journal of Cosmology …, 2022, https://doi.org/10.1088/1475-7516/2022/07/020.
20. D. Milner, J. Wesevich, L. Nikodym, V. Nasri, and ..., "Improved blast capacity of pre-engineered metal buildings using coupled CFD and FEA modeling," Journal of Loss …, 2018, [Online]. Available: https://www.sciencedirect.com/science/article/pii/S0950423018300949